UNIVERSITÀ DEGLI STUDI DI PALERMO

Dottorato in MEDICINA CLINICA E SCIENZE DEL COMPORTAMENTO
Dipartimento Biomedico di Medicina Interna e Specialistica (DiBiMIS)
Settore Scientifico Disciplinare Med/36

Performance of Gd-BOPTA Magnetic Resonance in the diagnosis of Hepatocellular Carcinoma, compared to histology after orthotopic liver transplantation.

IL DOTTORE
Dr. Giuseppe Mamone

IL COORDINATORE
Prof. Antonio Pinto

IL TUTOR
Prof. Giuseppe Brancatelli

CICLO XXIX
ANNO CONSEGUIMENTO TITOLO 2017

UNIVERSITÀ DEGLI STUDI DI PALERMO

INDICE

Introduction……..pag.3

Material and Methods……..pag.5

Results……..pag.12

Conclusion……..pag.22

References……..pag.28

INTRODUCTION

Hepatocellular carcinoma (HCC) is the sixth commonest cancer worldwide with the fastest rising cause of cancer-related deaths and a sharp increase in incidence over the past three decades [1].

The mortality rate of HCC is almost equal to the incidence rate, this reflects the lack of effective treatment at diagnosis, especially in advanced HCC [2].

Patients at a high risk of HCC should therefore undergo rigorous screening in order to detect HCC in its early form, at a stage where curative intervention is possible.

Diagnosis of HCC is most often possible through cross-sectional imaging alone, with histological analysis being the exception and not the rule.

In high risk patients, nodules larger than 1 cm showing arterial enhancement and venous washout on post-contrast multidetector-row computed tomography (MDCT) or magnetic resonance imaging (MRI) are diagnosed as HCC, as per the American Association for the Study of Liver Diseases (AASLD)

and European Association for the Study of the Liver-European Organisation for Research and Treatment of Cancer (EASL-EORTC) practice guidelines [3; 4].

This pattern is highly specific (close to 100%), but not as sensitive [5].

Our aim was to retrospectively review MRI studies performed with hepatobiliary contrast media in patients harbouring histologically proven HCCs on their liver explant post transplantation, and to identify the best combination of MRI imaging features useful in HCC diagnosis.

MATERIAL AND METHODS

Study population.

A total of 595 patients underwent liver transplantation between August 2004 and September 2012 in our hospital (ISMETT, Mediterranean Institute for Transplantation and Advanced Specialized Therapies, Palermo, Italy).

An interdependent query against our electronic health records and RIS database showed that 162 subjects also had MRI within the 90 days preceding surgery. A total of 65 patients were excluded. Of these, 34 underwent liver transplantation for indications other than cirrhosis with or without HCC, 22 had an MR examination which did not include the hepatobiliary phase, 5 had liver MRI performed using other contrast media, 3 had an inadequate scan due to excessive motion artefact, and one patient was transplanted outside the Milan criteria. The imaging evaluation was performed at a mean of 41.7±25.4 days prior to liver transplantation. 46 patients had undergone adjuvant percutaneous therapy for HCC (transarterial chemoembolization n=43, radiofrequency

ablation n=2, combination of TACE and RFA n=1). Our final study cohort consisted of 97 consecutive subjects (Table 1).

Table 1: Patient characteristics.

Parameter	**Value**
Mean age (years)	58.5 (range: 41-70)
Sex ratio (M:F)	78:19
Aetiology of cirrhosis (*n*)	
Hepatitis C	57
Hepatitis B	22
Cryptogenic	5
Alcohol	3
Hepatitis B and C	2
Other	8
α-feto-protein level (ng/mL)	
≤ 10	45
11-100	32
101-399	15
≥ 400	5
MELD score (*n*)	
≤ 9	28
10-14	46
15-19	13
20-24	4
≥ 25	6
MELDNa score (*n*)	
≤ 9	21
10-14	35
15-19	25
20-24	8
≥ 25	8

Note: *n* = number of patients, MELD is the Model for End-Stage Liver Disease, MELD-Na = integrated MELD model including serum sodium.

MR protocol.

Our MR examinations were performed using a super-conducting magnet operating at 1.5 Tesla (Signa 1.5T HDxt, GE Healthcare, Milwaukee, WI, USA), with an 8-channel phased-array body coil centered on the liver.

MR imaging was performed before and after Gd-BOPTA (MultiHance, Bracco SpA, Milan, Italy) injection (0.1 mmol/kg; 2.4 mL/s) through an 18-21 gauge peripheral intravenous cannula using an automated dual-chamber injector (Spectris MR Injector; Medrad , PA, USA), followed by a 10 to 15 mL saline flush.

The full hepatobiliary protocol is detailed in Table 2.

Table 2: Technical parameters of the different sequences in our institutional MRI Liver protocol.

Sequence	Scan Matrix	Slice Thickness (mm)	Intersection gap (mm)	Repetition time (msec) / Echo Time (msec)	Flip Angle	Echo Train Length	Fat suppression	FOV (cm)	Reconstruction matrix (ZIP)
Breath-hold bSSFP (FIESTA)	352x224	5	0.5	4.2 / 2.1	110	90	Spectral saturation	40x40	512
Breath-hold T2-weighted SSFSE	384x224	5	0.5	756 / 102	90	14	No	40x40	512
Breath-hold T2-weighted SSFSE fat sat	288x224	5	0.5	701 / 120	90	14	Spectral saturation , Asset acceleration factor 2, average 1	40x40	512
T2-weighted SPAIR	416x256	5	0.5	10000 / 120	90	13	Asset factor 1.75 , with spectral adiabatic inversion recovery	40x40	512
3D T1-weighted in-phase and out-of-phase	320x192	4	Interleave	150 / 2.2-4.2	80	n/a	ARC factor 1	40x40	512
DWI b=400/800	128x128	5	0.5	8000 / 2.2	90	n/a	Asset factor 2 with spectral saturation	40x40	512
T1-weighted FSPGR LAVA	384x224	4	Voxel continum	1.8 /4.2	12	n/a	ARC factor 1,75 with selective spectral saturation	40x32	409.6

Note:
FIESTA = Fast Imaging Employing Steady State Acquisition
SSFSE = Single Shot Fast Spin Echo
SPAIR = SPectral Attenuated Inversion Recovery
DWI = Diffusion Weighted Imaging
FSPGR = fast spoiled gradient echo
LAVA = Liver Acquisition with Volume Acquisition
ZIP = Zero Fill Interpolation Processing

Histopathological assessment.

Histopathological examination of the explanted livers was considered the gold standard.

Explanted livers were fixed in formalin and serially sliced in the transverse plane at 5 mm intervals corresponding as closely as possible to the imaging planes, as per institutional protocol. Nodule size, nodule location (as per Couinaud classification), capsule, micro and macro-vascular, perineural invasion and nodal involvement were recorded.

All lesions were sampled, fixed in formalin, embedded in paraffin, and cut into 3-4-micron-thick sections.

The histopathology of all nodules was reviewed by a pathologist with 13 years' experience in liver histopathology, blinded to the imaging findings. Nodules were classified into regenerative nodules, low-grade dysplastic nodules (LGDN), high grade dysplastic nodules, and grade I-III hepatocellular carcinoma nodules as per Edmondson and Steiner criteria [6; 7].

Image analysis.

A nodule-by-nodule analysis was jointly performed by two board-certified radiologists (with 5 and 11 years of experience in abdominal imaging, respectively) blinded to the reported radiological findings.

Both radiologists had full access to the histopathology report. In cases where more than one Gd-BOPTA enhanced MRI was performed per patient during the three months preceding liver transplantation, only the latest examination was taken into consideration.

Images were interpreted on a work station with a LCD 21" display with spatial resolution of 2 x 5 megapixels (Barco, Kortrijk, Belgium) running Centricity Picture Archiving & Communications System (PACS) version 3.2 (GE Healthcare). The signal intensity (hypo-, iso-, and hyper-intense) of the HCC nodules under study was analysed on all sequences performed as part of our institutional protocol.

Arterial enhancement following injection of contrast was graded as either mild to moderate, or intense.

A ‘pseudocapsule’ was defined as a peri-nodular rim which enhances in the venous phases, or appears hypointense in the hepatobiliary phase [8; 9].

Statistical analysis.

Statistical analysis was performed by a biostatistician.

A multiple logistic regression analysis was performed following pathological/radiological correlation, and the Odds Ratio (OR) was calculated for every parameter analyzed and adjusted for nodule size.

Confidence Intervals (CI) were reported at 95%, and a p value of less than 0.05 was considered to be statistically significant in all statistical tests.

Statistical analysis were performed using Stata 13.0 (StataCorp, College Station, TX, USA) and R version 3.0.0 (R Development Core Team, Vienna, Austria) [10].

RESULTS

Histopathological findings.

A total of 240 HCC nodules were reported in the 97 patients included in this study.

47 HCCs had massive necrosis (intra-tumoral necrosis of ≥ 90%) due to previous percutaneous locoregional therapy. These HCCs were eliminated from subsequent analysis.

This resulted in a total of 193 HCCs, in 77 patients.

Seventeen patients had 1 HCC nodule; twenty-two patients had 2 nodules; twelve patients had 3 nodules; and twenty-six patients had more than 3 nodules.

Fig.1 shows some pathological examination with HCC.

The mean HCC diameter was 17.8±10.2 mm.

Tumour size was ≤10 mm in 28 HCC, 10–20 mm in 107 HCC and ≥20 mm in 58 HCC.

Microvascular invasion was detected in 60.6 % (117/193) nodules.

Forty-eight patients had nodules other than HCC (68 regenerative nodules, 8 low-grade dysplastic nodules, 19 high-grade dysplastic nodules, 2 cholangiocarcinomas, 1 necrotic nodule).

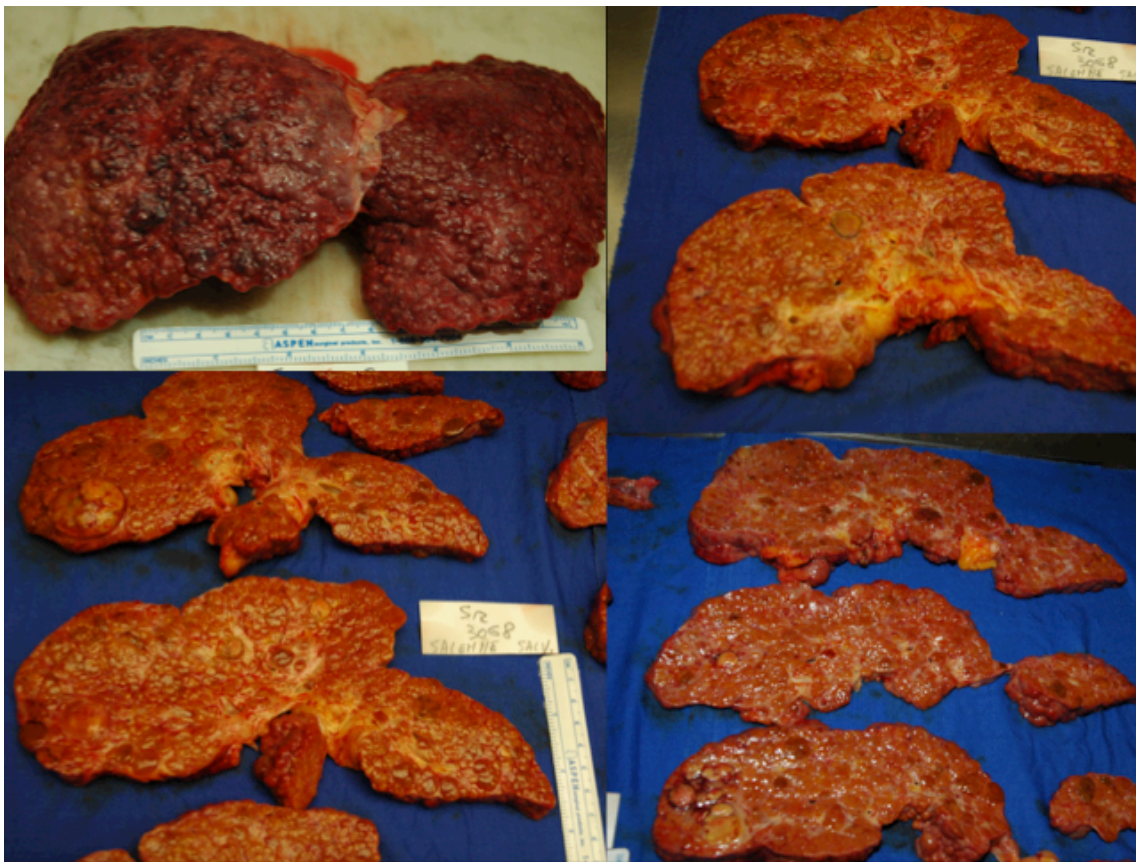

Fig.1: pathological examination resulting in liver cirrhosis and HCC.

MRI findings.

Of the 193 HCCs seen on histopathology, 24.9% (48/193) were not detectable on imaging.

The signal intensity of the remaining 145 HCCs were analysed on all sequences performed as part of our institutional protocol.

The Odds Ratio (OR) was calculated for every parameter analysed and adjusted for nodule size, this is displayed in Tables 3 and 4, and also in Figure 2.

MRI features that favour a diagnosis of HCC are shown in blue, while the findings that suggest a diagnosis of non-HCC are shown in red, with the respective ORs.

Visualisation of a pseudocapsule on the venous or hepatobiliary phases (Fig.3) produced the highest OR (35.3, $p<0.000$).

As expected, intense (OR 10.9, $p<0.000$) or moderate (OR 2.2, $p=0.003$) arterial enhancement and hypointensity on the portal venous (OR 14.3, $p<0.000$) or equilibrium (OR 15.9, $p<0.000$) phases were found to predict HCC (Fig.4).

In addition, nodules showing hypointensity on the hepatobiliary phase (Fig.5) and mild-moderate T2 hyperintensity (Fig.6) were also highly likely to represent HCC. In the former, an OR of 10.2 was observed ($p<0.000$).

The OR was 14.3 in non-FS T2 weighted sequences, and 10.2 in FS T2 weighted sequences ($p<0.000$).

Table 3: MRI features that favour HCC.

MR finding	Prevalence in HCC	OR	p value
Pseudocapsule	58 (17.2%)	35.33	<0.000
↓ equilibrium phase	80 (55.2%)	15.93	<0.000
↓ portal venous phase	58 (17.2%)	14.35	<0.000
↑ T2	45 (31.0%)	14.30	<0.000
Intense arterial enhancement	59 (40.7%)	10.94	<0.000
↓ hepatobiliary phase	80 (55.2%)	10.23	<0.000
↑ T2 with spectal fat suppression	33 (22.8%)	10.16	<0.000
↓ T1 (out-of-phase)	34 (23.4%)	6.66	<0.000
↑ portal venous phase	19 (13.1%)	6.10	0.004
↓ T1 (in-phase)	18 (12.4%)	3.21	0.042
↔ T1 (in-phase)	93 (64.1%)	2.62	<0.000
↔ T1 (out-of-phase)	89 (61.4%)	2.36	<0.000
Moderate arterial enhancement	50 (34.5%)	2.17	0.003

OR = Odds Ratio
↔ Isointense
↓ Hypointense
↑ Hyperintense

Table 4: MRI features that favour non-HCC.

MR finding	Prevalence in HCC	OR	p value
↔ hepatobiliary phase	56 (38.6%)	0.63	0.007
↔ portal venous phase	68 (46.9%)	0.62	0.003
↔ equilibrium phase	58 (40%)	0.53	<0.000
↑ hepatobiliary phase	9 (6.2%)	0.45	0.047
↑ T1 IP	34 (23.4%)	0.45	<0.000
No arterial enhancement	22 (15.2%)	0.32	<0.000
↑ T1 OP	22 (15.2%)	0.30	<0.000
↓ T2 FS	10 (6.9%)	0.28	<0.000
↓ T2	9 (6.2%)	0.25	<0.000

↔ Isointense
↓ Hypointense
↑ Hyperintense

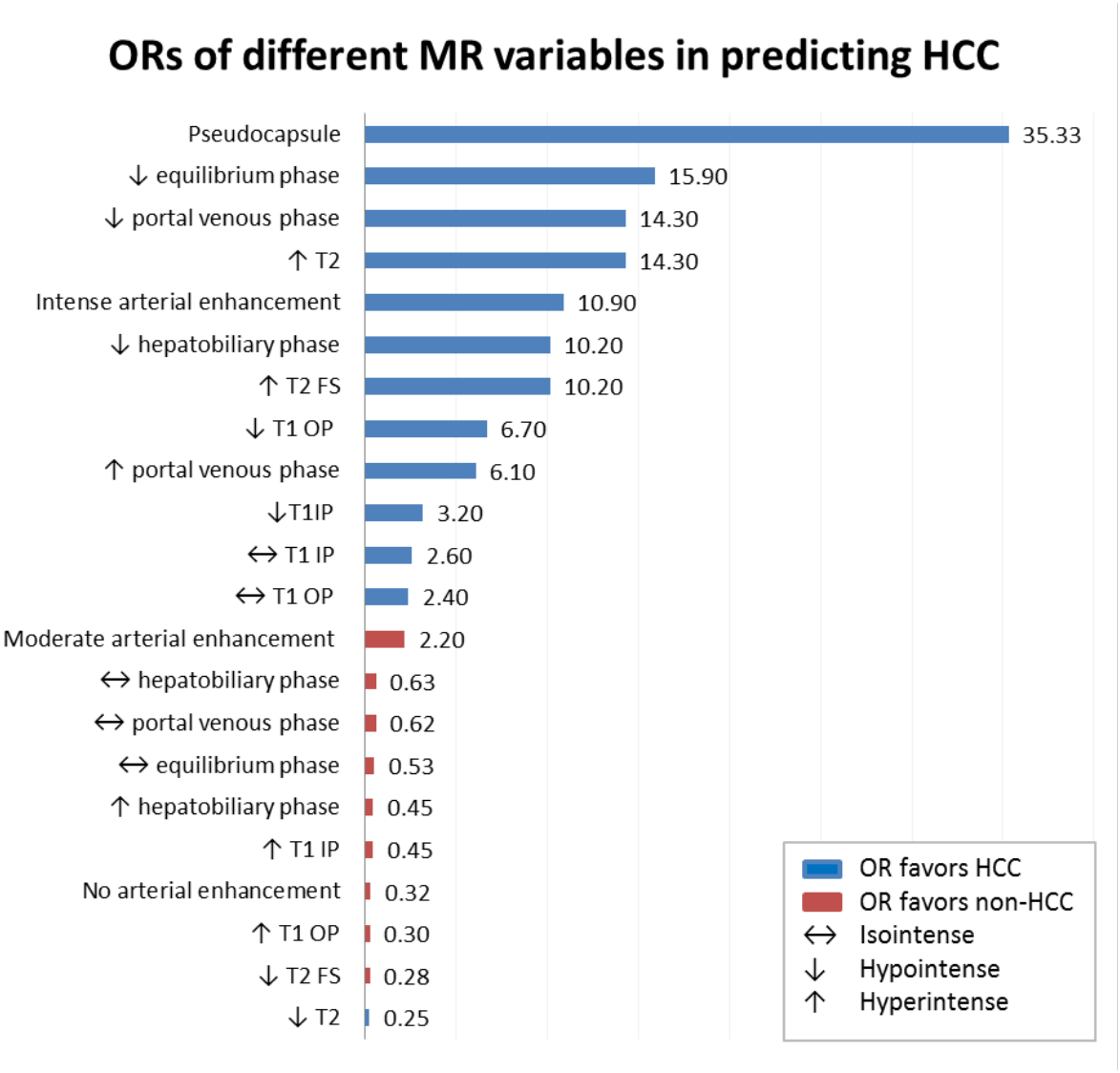

Fig.2: MR variables predicting HCC.

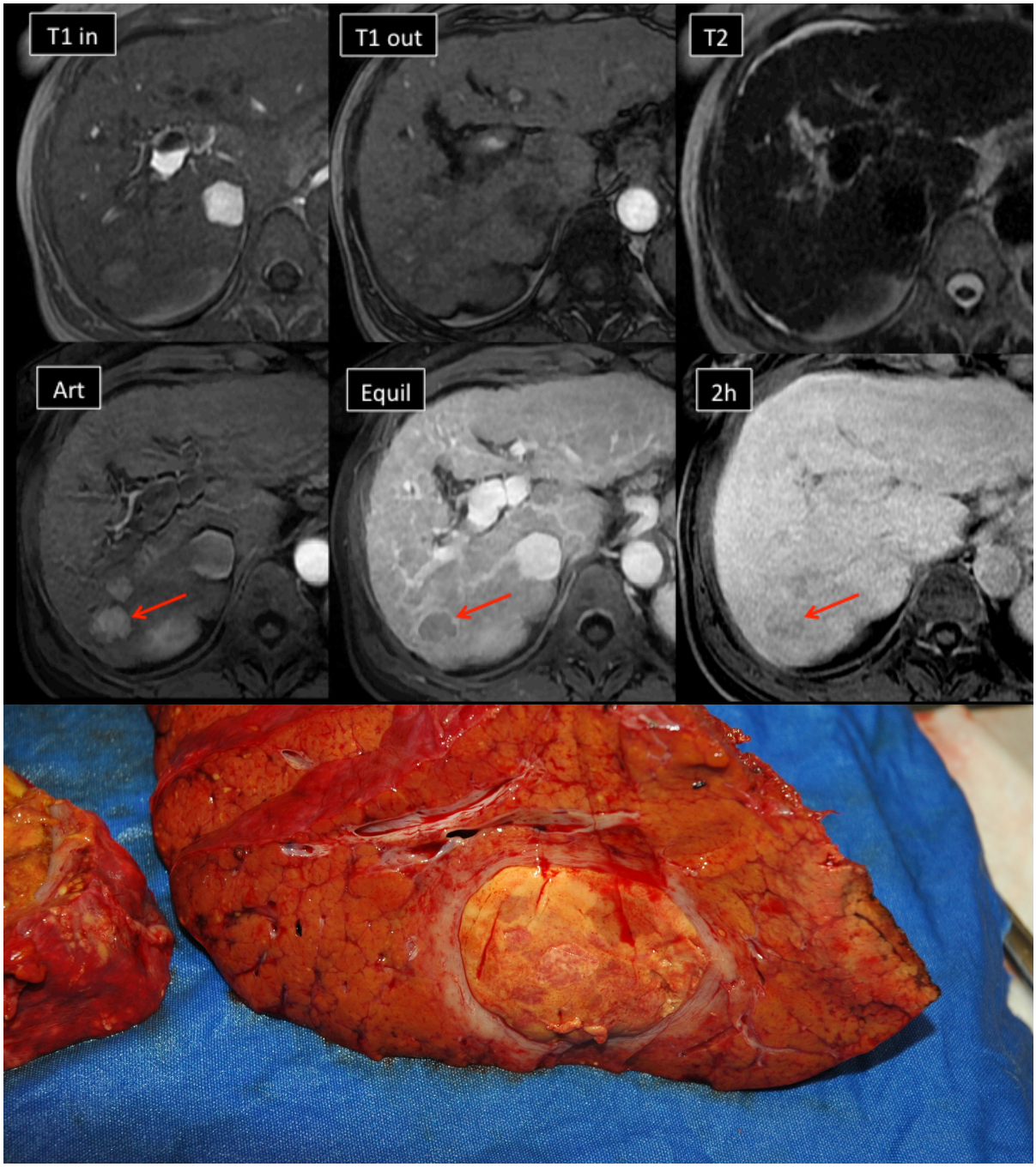

Fig.3: HCC with wash-in and wash-out; notice the pseudocapsule on equilibrium phase and on pathological examination.

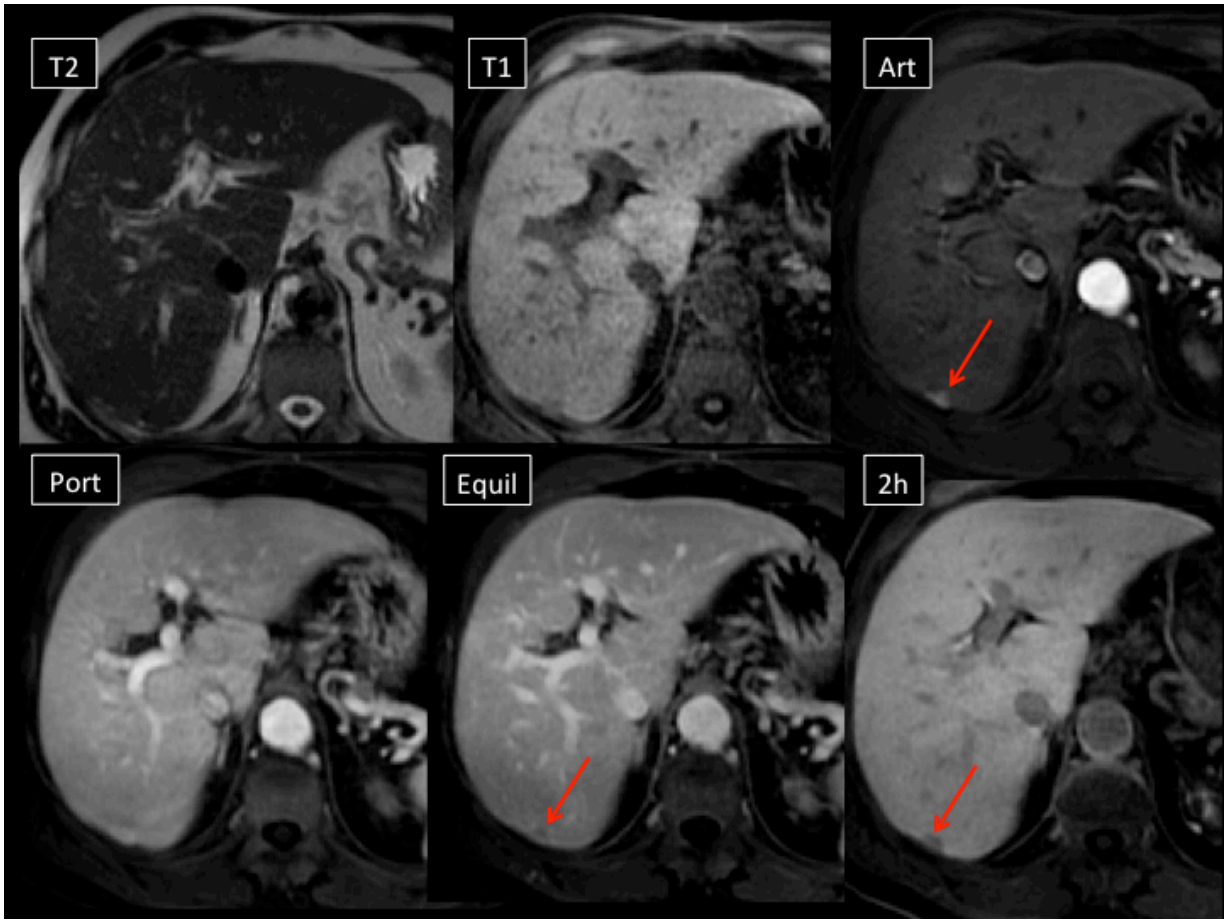

Fig.4: HCC with typical pattern (wash-in and wash-out). Notice the hypointensity on hepatobiliary phase.

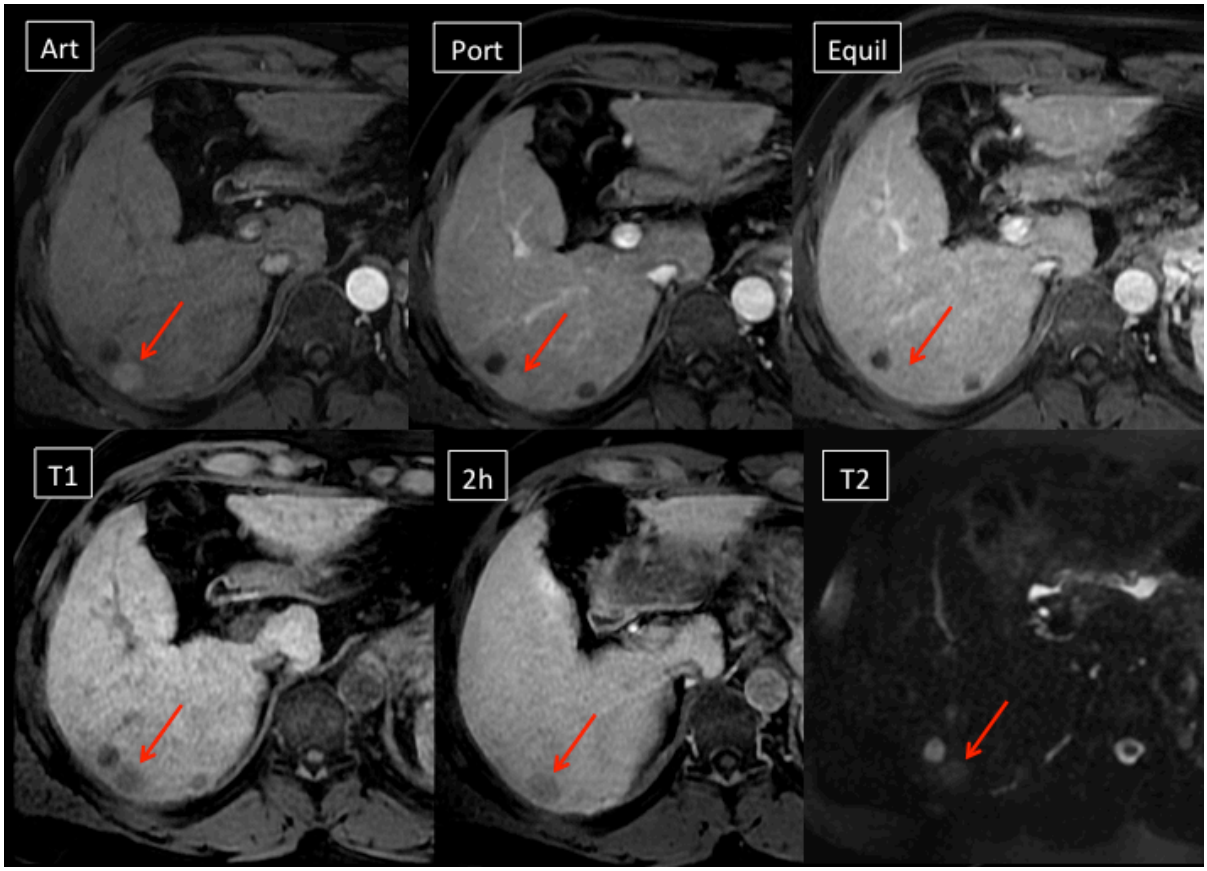

Fig.5: HCC with wash-in but without wash-out; however, the lesion showed hypointensity on hepatobiliary phase.

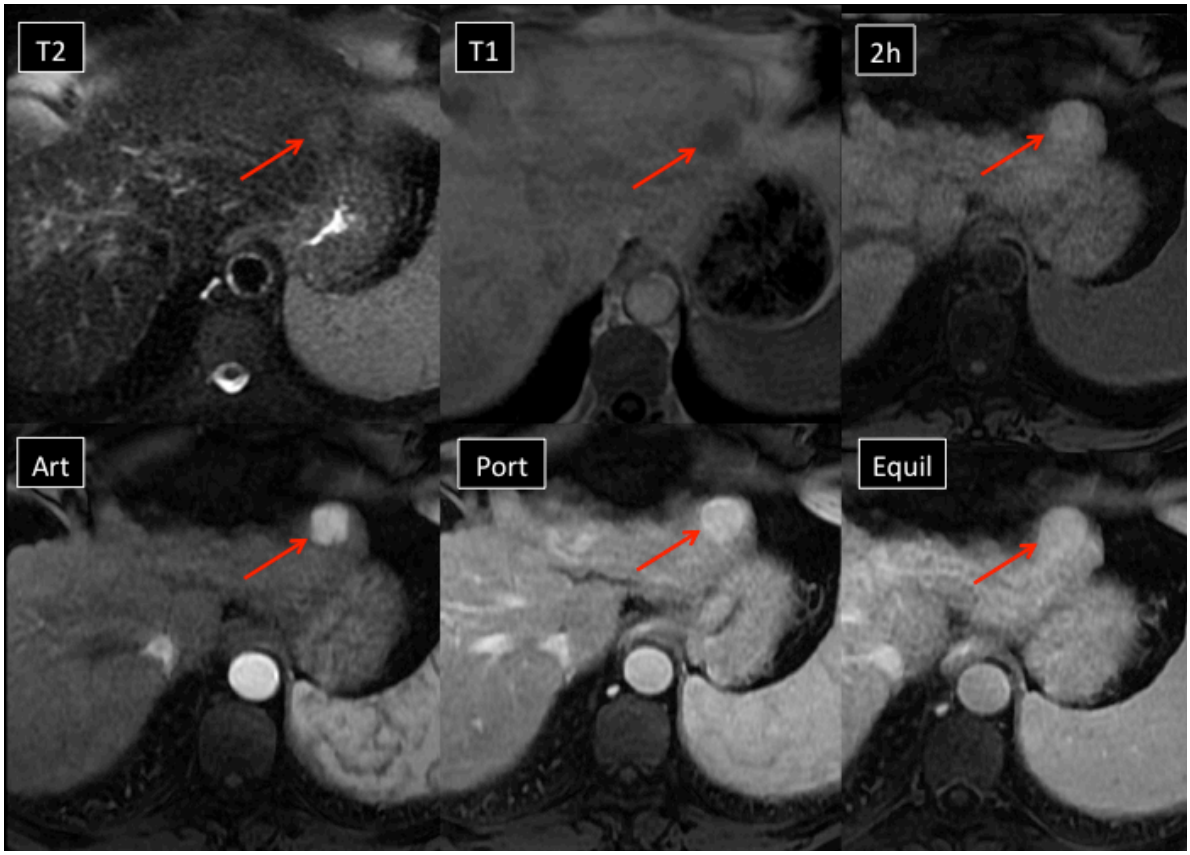

Fig.6: HCC with wash-in but without wash-out on equilibrium and hepatobiliary phases; however, the lesion showed hyperintensity on T2w sequence.

CONCLUSION

MRI, unlike MDCT, is not simply a multi-phase post-contrast study.

An array of T1 and T2 weighted sequences are performed, with the aim of portraying the inherent biological characteristics of the tissue under study, the vascular enhancement dynamics, and presence or absence of hepatocyte function when hepatobiliary contrast media are used.

Our study confirms the usefulness of arterial enhancement and venous washout, as per the AALSD and EASL-EORTC guidelines, and also justifies incorporating hepatobiliary phase hypointensity in the diagnosis of HCC [11; 12].

We have also shown that in patients with a high risk of HCC, nodules showing a pseudocapsule, mild-moderate T2 hyperintensity, and T1 iso to hypointensity, are likely to represent HCC.

On the other hand, imaging features which point towards non-HCC include T2 hypointensity, T1 hyperintensity, no arterial enhancement, and hyperintensity on the hepatobiliary phase.

The current AASLD and EASL-EORTC practice guidelines rely exclusively on the contrast enhancement characteristics of HCC. In both guidelines, nodules over 1 cm in diameter showing wash-in of contrast during the arterial phase, followed by washout of contrast during the portal or delayed venous phase on either MDCT or MRI, should be regarded as HCC in patients with cirrhosis from any aetiology, or in non-cirrhotic patients with chronic hepatitis B infection.

There is no mention of hepatobiliary MRI contrast media in the AASLD and/or EASL-EORTC guidelines, in the latest updates published in 2011 and 2012, respectively.

The Liver Imaging Reporting and Data System (LI-RADS) utilises 'ancillary features' that favour malignancy or benignity, and incorporates use of hepatobiliary contrast agents [13].

LI-RADS ancillary features that favour malignancy include mild-moderate hepatobiliary phase hypointensity, T2

hyperintensity, restricted diffusion, intralesional fat and lesional haemorrhage.

The presence of a pseudocapsule is a major feature in diagnosing HCC, together with venous washout and interval growth. To date, LI-RADS has not been incorporated in the AALSD guidelines.

In Japan HCC surveillance is performed by MRI performed with the use of hepatobiliary contrast media (Gd-EOB).

MDCT is only performed whenever MRI is not available as per the Japan Society of Hepatology (JSH) practice guidelines [14].

There is no dimensional cut-off above which HCC can be diagnosed.

Nodules showing arterial enhancement, no venous washout, and hypointensity on the hepatobiliary phase are also diagnosed as HCC in the JSH guidelines.

This rigorous approach is resulting in identification of potentially curable early-stage HCC – which amount to around 62% of the patients diagnosed with HCC in Japan (only

around 30% of patients diagnosed with HCC are eligible for curable treatment in the West) [15].

Apart from the intrinsic limitations of any retrospective study, our study had the following limitations.

The most evident limitation is the potential miscorrelation between the histology section planes of liver explants and the MRI imaging section.

We tried to reduce the risk of miscorrelation by measuring the distance between the lesion and liver capsule, and coupling this with segmental anatomy when correlating histological and radiological data.

A significant limitation of our study is that DWI was only included in the standard protocol during the actual study period, and a significant number of the MRIs included in our study either lacked DWI, or had diffusion imaging performed with different b values (400, 600, or 800).

A reliable statistical analysis could not be performed for these reasons.

Hwang J et al recently reported the potential of utilising diffusion weighted imaging (DWI) to distinguish hypovascular HCC from dysplastic nodules [16].

This was noted by the study group of Renzulli M et al, that proposed the inclusion of DWI in the surveillance algorithm already being followed in Japan [17].

Another limitation is that of having an artificial increase in sensitivity due to our selected patient population with a higher pre-test prevalence of HCC than that present in the general population.

Finally, the pathological assessment done in this study was based on the International Working Party (1995) given that this study included data preceding the updated consensus published in 2009 by the International Consensus Group for Hepatocellular Neoplasia (ICGHN) [18].

In conclusion, MRI might provide auxiliary findings that facilitate diagnosis of HCC in nodules lacking the typical enhancement pattern.

The full potential of MRI should be exploited in patients with chronic liver disease, and any update to the existing European HCC surveillance guidelines should provide detailed information on a cross-platform MRI protocol aimed at detecting early HCC, with inclusion of hepatobiliary contrast media.

REFERENCES

1) El-Serag HB, Kanwal F (2014) Epidemiology of hepatocellular carcinoma in the United States: where are we? Where do we go? Hepatology 60:1767-1775
2) Bruix J, Gores GJ, Mazzaferro V (2014) Hepatocellular carcinoma: clinical frontiers and perspectives. Gut 63:844-855
3) Bruix J, Sherman M, American Association for the Study of Liver D (2011) Management of hepatocellular carcinoma: an update. Hepatology 53:1020-1022
4) European Association For The Study Of The L, European Organisation For R, Treatment Of C (2012) EASL-EORTC clinical practice guidelines: management of hepatocellular carcinoma. J Hepatol 56:908-943
5) Luca A, Caruso S, Milazzo M et al (2010) Multidetector-row computed tomography (MDCT) for the diagnosis of hepatocellular carcinoma in cirrhotic candidates for liver transplantation: prevalence of radiological vascular patterns and histological correlation with liver explants. Eur Radiol 20:898-907
6) Edmondson HA, Steiner PE (1954) Primary carcinoma of the liver: a study of 100 cases among 48,900 necropsies. Cancer 7:462-503
7) International Working P (1995) Terminology of nodular hepatocellular lesions. Hepatology 22:983-993
8) Ishigami K, Yoshimitsu K, Nishihara Y et al (2009) Hepatocellular carcinoma with a pseudocapsule on gadolinium-enhanced MR images: correlation with histopathologic findings. Radiology 250:435-443
9) Dioguardi Burgio M, Picone D, Cabibbo G, Midiri M, Lagalla R, Brancatelli G (2016) MR-imaging features of hepatocellular

carcinoma capsule appearance in cirrhotic liver: comparison of gadoxetic acid and gadobenate dimeglumine. Abdom Radiol (NY) 41:1546-1554

10) R Development Core Team. R: A language and environment for statistical computing. Vienna: R Foundation for Statistical Computing, 2011.
11) Cortis K, Liotta R, Miraglia R, Caruso S, Tuzzolino F, Luca A (2016) Incorporating the hepatobiliary phase of gadobenate dimeglumine-enhanced MRI in the diagnosis of hepatocellular carcinoma: increasing the sensitivity without compromising specificity. Acta Radiol 57:923-931
12) Faletti R, Cassinis MC, Fonio P et al (2015) Multiparametric Gd-EOB-DTPA magnetic resonance in diagnosis of HCC: dynamic study, hepatobiliary phase, and diffusion-weighted imaging compared to histology after orthotopic liver transplantation. Abdom Imaging 40:46-55
13) Hope TA, Fowler KJ, Sirlin CB et al (2015) Hepatobiliary agents and their role in LI-RADS. Abdom Imaging 40:613-625
14) Kudo M, Matsui O, Izumi N et al (2014) JSH Consensus-Based Clinical Practice Guidelines for the Management of Hepatocellular Carcinoma: 2014 Update by the Liver Cancer Study Group of Japan. Liver Cancer 3:458-468
15) Kudo M, Izumi N, Sakamoto M et al (2016) Survival Analysis over 28 Years of 173,378 Patients with Hepatocellular Carcinoma in Japan. Liver Cancer 5:190-197
16) Hwang J, Kim YK, Jeong WK, Choi D, Rhim H, Lee WJ (2015) Nonhypervascular Hypointense Nodules at Gadoxetic Acid-enhanced MR Imaging in Chronic Liver Disease: Diffusion-weighted Imaging for Characterization. Radiology 277:309

17) Renzulli M, Golfieri R, Bologna Liver Oncology G (2016) Proposal of a new diagnostic algorithm for hepatocellular carcinoma based on the Japanese guidelines but adapted to the Western world for patients under surveillance for chronic liver disease. J Gastroenterol Hepatol 31:69-80
18) International Consensus Group for Hepatocellular NeoplasiaThe International Consensus Group for Hepatocellular N (2009) Pathologic diagnosis of early hepatocellular carcinoma: a report of the international consensus group for hepatocellular neoplasia. Hepatology 49:658-664.